Materials Transactions, Vol. 46, No. 6 (2005) pp. 1318 to 1323

Thermal Cycle Resistance of Yttria Stabilized Zirconia Coatings Prepared by MO-CVD

Rong Tu and Takashi Goto

Institute for Materials Research, Tohoku University, Sendai 980-8577, Japan

Yttria stabilized zirconia (YSZ) coatings containing 0 to 9.5 mol% Y_2O_3 were prepared on Hastelloy-XR alloys by metal-organic chemical vapor deposition (MO-CVD), and the effect of Y_2O_3 content on thermal cycle resistance was investigated in the temperature intervals from 600 to 1273 K and from 600 to 1373 K in air. In the 600–1273 K interval, delamination after 1200 cycles had not occurred for any of the Y_2O_3 contents of YSZ coatings. In the 600–1373 K interval, the YSZ coatings containing 0, 0.5 and 9.5 mol% Y_2O_3 suffered partial delamination after 1200 cycles, while no delamination was observed for the YSZ coatings containing 4 mol% Y_2O_3. During the thermal cycles, thermally grown oxide (TGO) layers consisting of inner Cr_2O_3 and outer $(Ni,Mn,Fe)(Fe,Cr)_2O_4$ spinel were formed at the YSZ coating/Hastelloy-XR substrate alloy interface. The delamination of YSZ coatings occurred at the alloy side near the TGO layer/Hastelloy-XR alloy interface.

(Received September 15, 2004; Accepted April 11, 2005; Published June 15, 2005)

Keywords: *thermal cycle resistance, yttria stabilized zirconia (YSZ) coatings, metal-organic chemical vapor deposition (MO-CVD), thermally grown oxide (TGO) layer, Hastelloy-XR alloy*

1. Introduction

Due to the strong demand for improvement of thermal efficiency, the gas turbine inlet temperature is increasing to more than 1773 K. However, the temperature to which turbine blades are subjected should be suppressed below 1273 K, mainly due to the limitation of the thermo-mechanical performance of Ni-based superalloys at higher temperatures. Thus, turbine blades are cooled by airflow and protected by thermal barrier coatings (TBCs). Yttria stabilized zirconia (YSZ) has been usually employed as a TBC because of its chemical inertness, low thermal conductivity and high thermal expansion coefficient compatible with superalloy substrates.[1,2] YSZ coatings for TBCs with a thickness of more than several hundred micrometers have been mainly fabricated by atmospheric plasma spraying (APS)[3] or electron-beam physical vapor deposition (EB-PVD).[4,5] APS can produce lamellar-structured YSZ coatings with low thermal conductivity; however, thermal cycles may cause interlayer cracking leading to delamination in a relatively short time. EB-PVD YSZ coatings exhibit good thermal cycle resistance owing to their columnar microstructure, but, unfortunately, the gas diffusion through intercolumnar gaps causes oxidation of the bond coat layer, resulting in delamination of such coatings.

Chemical vapor deposition (CVD) has been widely used to prepare YSZ thin films for application mainly as an oxide solid electrolyte and a buffer layer for high-temperature superconductors.[6,7] The deposition rates of YSZ films by CVD have generally been several $\mu m\,h^{-1}$, too low for their application as TBCs.[8,9] Recently, several groups have reported high deposition rates of YSZ films of more than $50\,\mu m\,h^{-1}$ by using MO-CVD,[10–12] and we have prepared YSZ films with deposition rates up to 108 μm h.[13] Therefore, the CVD process may be applicable to TBCs. However, no thermal cycle resistance of CVD YSZ coatings has been reported. In the present study, CVD YSZ coatings were prepared directly on Hastelloy-XR alloy without a bond coat layer at high deposition rates and their thermal cycle resistance was investigated. In particular, the effect of Y_2O_3 content on the thermal cycle performance and the growth characteristics of the oxide layer between the CVD YSZ coating and the Hastelloy-XR alloy were studied.

2. Experimental

YSZ coatings were prepared by a vertical cold-wall type CVD apparatus using $Zr(dpm)_4$ and $Y(dpm)_3$ precursors. Hastelloy-XR alloy (49Ni–22Cr–18Fe–9Mo–0.9Mn–0.3Si in mass%) disks, 10 mm in diameter and 1 mm in thickness, were used as substrates. The Y_2O_3 content in YSZ coatings was varied from 0 to 10 mol%. The Y_2O_3 content was determined by electron probe microanalysis (EPMA) accompanying lattice parameter measurement by X-ray diffraction (XRD). Details of the deposition conditions have been reported elsewhere.[14]

Thermal cycle experiments were conducted by using an infrared lamp furnace. The specimens were heated up to 1273 or 1373 K in air at a rate of $5\,K\,s^{-1}$ and then cooled to 600 K within 0.6 ks after being kept at these temperatures for 0.6 ks. Using a thermocouple (R-type) in direct contact with the substrates, it was confirmed that the substrate temperature of the alloy was raised to a specific temperature within a few seconds. This thermal cycle was performed up to 1200 cycles. Figure 1 demonstrates the pattern of thermal cycles. The change of crystal structure after the thermal cycles was studied by X-ray diffraction (XRD). The microstructure change was examined by scanning electron microscopy (SEM).

3. Results and Discussion

Figure 2 presents the appearances of CVD YSZ coatings on Hastelloy-XR alloys after 1200 cycles in the 600–1273 K interval. No delamination was observed in any of the specimens. The appearances of CVD YSZ coatings after 800 and 1200 cycles in the 600–1373 K interval are shown in Figs. 3 and 4, respectively. The thermal cycle resistance of YSZ coatings significantly depended on the Y_2O_3 content. ZrO_2 coatings not containing Y_2O_3 were partially delami-

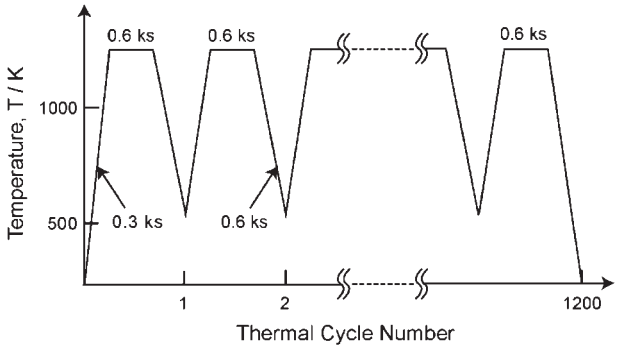

Fig. 1 Thermal cyclic pattern for YSZ coatings on Hastelloy-XR alloy.

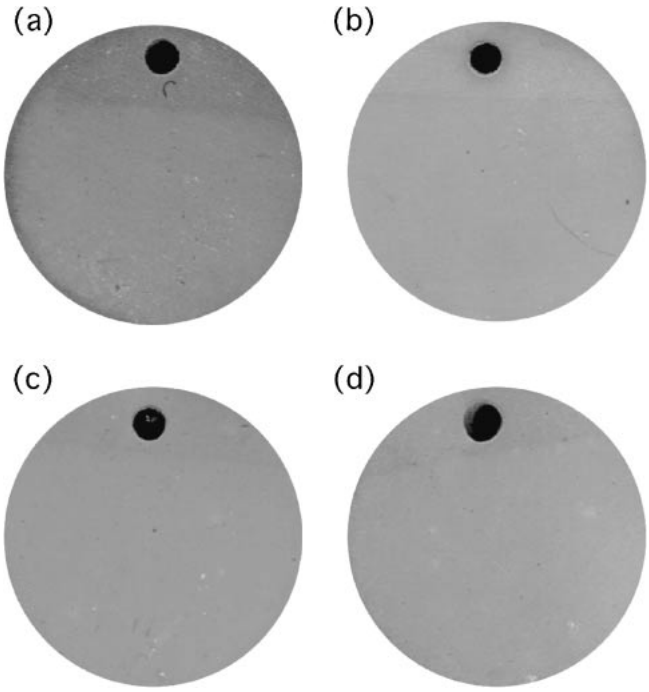

Fig. 2 Appearance of YSZ coatings on Hastelloy-XR alloy in the 600–1273 K interval after 1200 cycles in air. (Y_2O_3 content: (a) 0, (b) 0.5, (c) 4, (d) 9.5 mol%)

nated after 800 cycles (Fig. 3(a)) and wholly delaminated after 1200 cycles (Fig. 4(a)). Although the YSZ coatings containing 0.5 and 9.5 mol% Y_2O_3 manifested no delamination after 800 cycles (Figs. 3(b) and (d)), partial delamination was observed after 1200 cycles (Figs. 4(b) and (d)). The YSZ coating containing 4 mol% Y_2O_3 nearly maintained its initial appearance after 1200 cycles (Fig. 4(c)). Since the sintered YSZ ceramics containing 4 mol% Y_2O_3 have a partially stabilized tetragonal structure, the crack propagation in the YSZ can be hindered by stress-induced transformation from tetragonal to monoclinic structure at the very top of cracks (transformation toughening).[15] It is also known that any transformation of YSZ coatings containing 4 mol% Y_2O_3 hardly occurs due to heat-treatment, thus resulting in good thermal shock resistance and adherence to substrates. Therefore, YSZ coatings, mainly containing 4 mol% Y_2O_3, are generally employed in commercial applications of APS and EB-PVD. In the present study, CVD YSZ containing 4 mol% Y_2O_3 was also found to have the best performance.

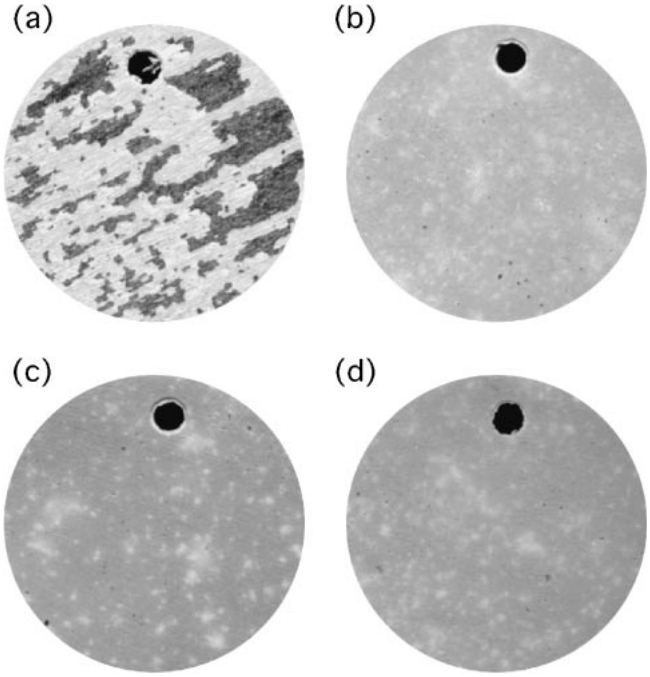

Fig. 3 Appearance of YSZ coatings on Hastelloy-XR alloy in the 600–1373 K interval after 800 cycles in air. (Y_2O_3 content: (a) 0, (b) 0.5, (c) 4, (d) 9.5 mol%)

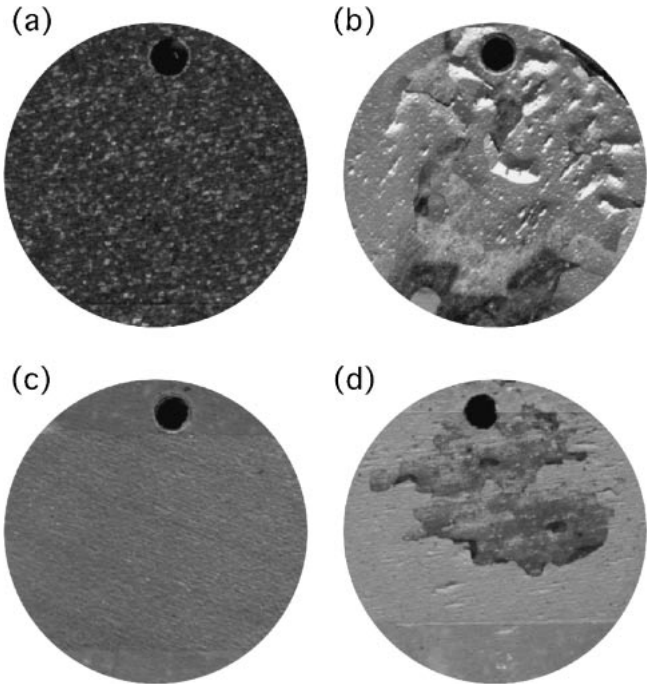

Fig. 4 Appearance of YSZ coatings on Hastelloy-XR alloy in the 600–1373 K interval after 1200 cycles in air. (Y_2O_3 content: (a) 0, (b) 0.5, (c) 4, (d) 9.5 mol%)

Figure 5 depicts the surface morphology of YSZ coatings after 1200 cycles in the 600–1373 K interval. The difference of the thermal expansion coefficient between the YSZ coating ($10 \times 10^{-6}\,K^{-1}$) and the Hastelloy-XR alloy ($16 \times 10^{-6}\,K^{-1}$) would result in the crack formation during the thermal cycles. The width of cracks increased with thermal cycles due to the shrinkage of the YSZ coating. Since it is known that

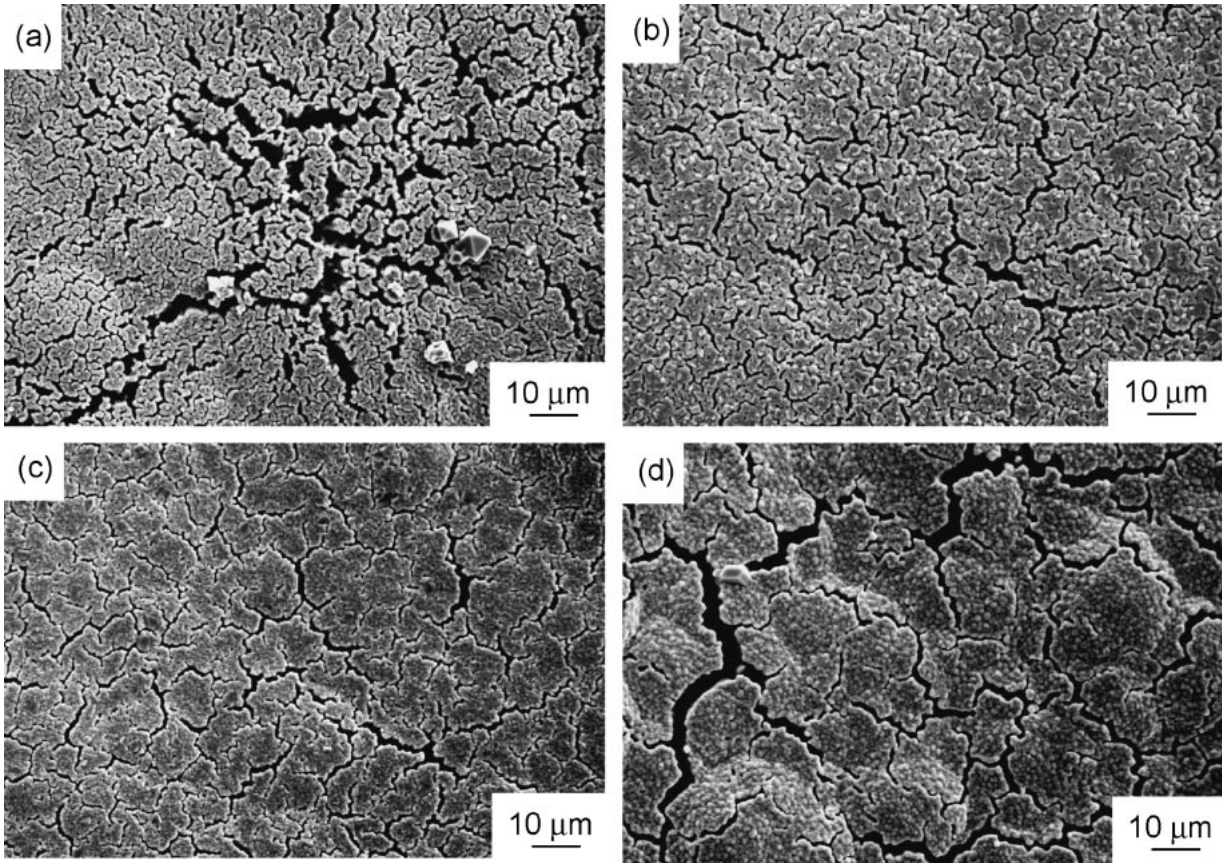

Fig. 5 Surface morphology of YSZ coatings on Hastelloy-XR alloy in the 600–1373 K interval after 1200 cycles in air. (Y_2O_3 content: (a) 0, (b) 0.5, (c) 4 and (d) 9.5 mol%)

YSZ coatings by APS, EB-PVD and CVD contain significant amounts of voids and pores, the sintering of YSZ grains easily occurs by heat treatment. The difference in the morphology of cracks in the YSZ coatings with different levels of Y_2O_3 content is probably related to the mechanical strength of YSZ coatings. In the YSZ coatings containing 0 and 0.5 mol% Y_2O_3 (Figs. 5(a) and (b)), the cracks were inhomogeneous with a mixture of large and small cracks. In the YSZ coating containing 4 mol% Y_2O_3 (Fig. 5(c)), small cracks were uniformly dispersed. In the YSZ coating containing 9.5 mol% Y_2O_3 (Fig. 5(d)), large cracks were dominantly formed. It can be seen that the formation of uniformly distributed small cracks could be effective to maintain good adherence between the YSZ coating and the alloy substrate after the severe thermal cycles.

Figure 6 demonstrates the XRD patterns of YSZ coatings before and after 1200 cycles in the 600–1373 K interval. Changes in the XRD patterns of YSZ coatings after thermal cycles depended on Y_2O_3 contents. The YSZ coatings containing 0 to 0.5 mol% Y_2O_3 were transformed from a mixture of monoclinic and tetragonal phases (Figs. 6(a) and (b)) to a monoclinic single phase (Figs. 6(e) and (f)). According to the phase diagram of the ZrO_2–Y_2O_3 system, the tetragonal phase is unstable and should have been transformed to the monoclinic phase at room temperature. However, residual stress in the YSZ coatings during the deposition process may stabilize the tetragonal phase. Garvie reported that the tetragonal phase became more stable with decreasing grain size due to excess surface energy.[16)]

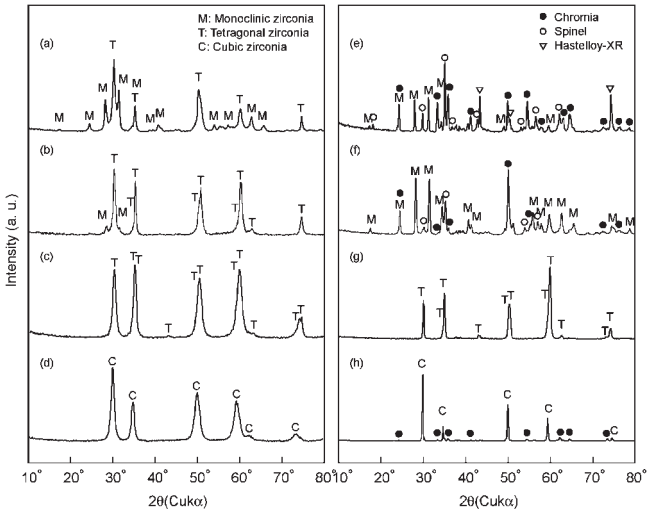

Fig. 6 XRD patterns of YSZ coatings on Hastelloy-XR alloy ((a)–(d)) and that in the 600–1373 K interval after 1200 cycles in air ((e)–(h)). (Y_2O_3 content: (a, e) 0, (b, f) 0.5, (c, g) 4, (d, h) 9.5 mol%)

Therefore, the tetragonal phase may be transformed to the monoclinic phase during the thermal cycles due to the grain growth and the release of residual stress. XRD peaks became sharper after the thermal cycles, suggesting grain growth. Cr_2O_3 and $(Ni,Mn,Fe)(Fe,Cr)_2O_4$ spinel were identified because the partial delamination of YSZ coatings resulted in exposure of the TGO layer. The YSZ coating containing

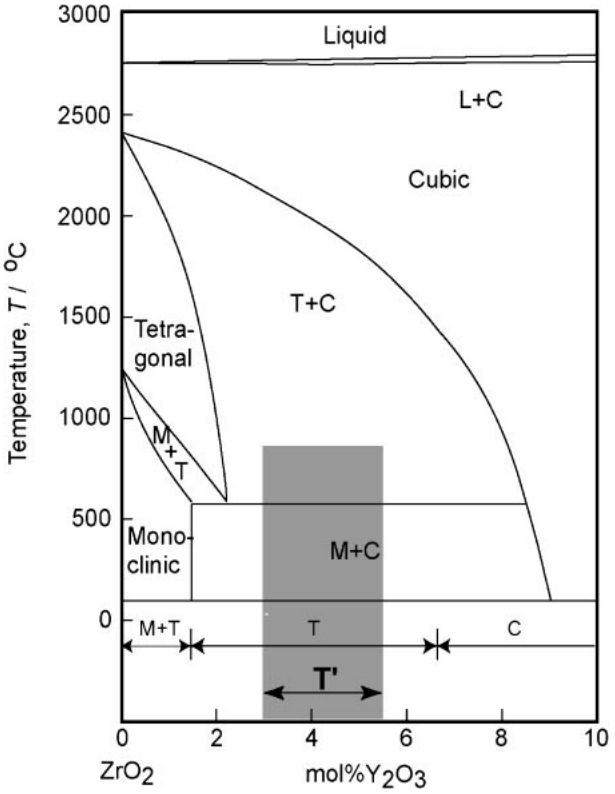

Fig. 7 Phase diagram of ZrO_2–Y_2O_3 system.[17)]

4 mol% Y_2O_3 was in a tetragonal single phase before and after the thermal cycles (Figs. 6(c) and (g)). The XRD peaks became sharper, suggesting the growth of YSZ grains by the thermal cycles. The YSZ coating containing 9.5 mol% Y_2O_3 was in a cubic single phase before the thermal cycles. No phase transformation occurred after the thermal cycles, but the peaks became sharper and small Cr_2O_3 peaks in the TGO layer were identified (Figs. 6(d) and (h)).

Figure 7 shows the phase diagram of the ZrO_2–Y_2O_3 system, indicating that the stable structure is dependent on Y_2O_3 content.[17)] The monoclinic, tetragonal and cubic phases are stable at room temperature when the Y_2O_3 content is less than 1.5 mol%, is between 1.5 and 9 mol% and is more than 9 mol% Y_2O_3, respectively. On the other hand, the YSZ coatings prepared by APS or CVD were a mixture of monoclinic and tetragonal phases at less than 1.5 mol% Y_2O_3, exhibited a tetragonal single phase between 1.5 and 6.5 mol% Y_2O_3, and had a cubic single phase at more than 6.5 mol% Y_2O_3.[18)] In the present study, the lattice parameter ratio (c/a) of the YSZ coating containing 4 mol% Y_2O_3 was 1.010, and no phase transformation occurred after the thermal cycles in the 600–1373 K interval (Figs. 6(c) and (g)). Heuer *et al.* named the tetragonal YSZ containing 3 to 6 mol% Y_2O_3 as the t′ phase, whose lattice parameter ratio (c/a) is close to 1 and in which the phase transformation from tetragonal to monoclinic cannot be observed after high temperature heat-treatment.[19)] The lattice parameters of the YSZ coatings containing 4 mol% Y_2O_3 in the present study were $a = 0.51097$ nm and $c = 0.51627$ nm ($c/a = 1.010$). These values are slightly different from those of the reported tetragonal YSZ ceramics ($a = 0.51087$ nm, $c = 0.51700$ nm, $c/a = 1.012$), and no phase transformation was observed after the thermal cycles in the 600–1373 K interval. The YSZ coatings containing 4 mol% Y_2O_3 prepared by the present CVD may be the t′ (non-transformable tetragonal) phase.

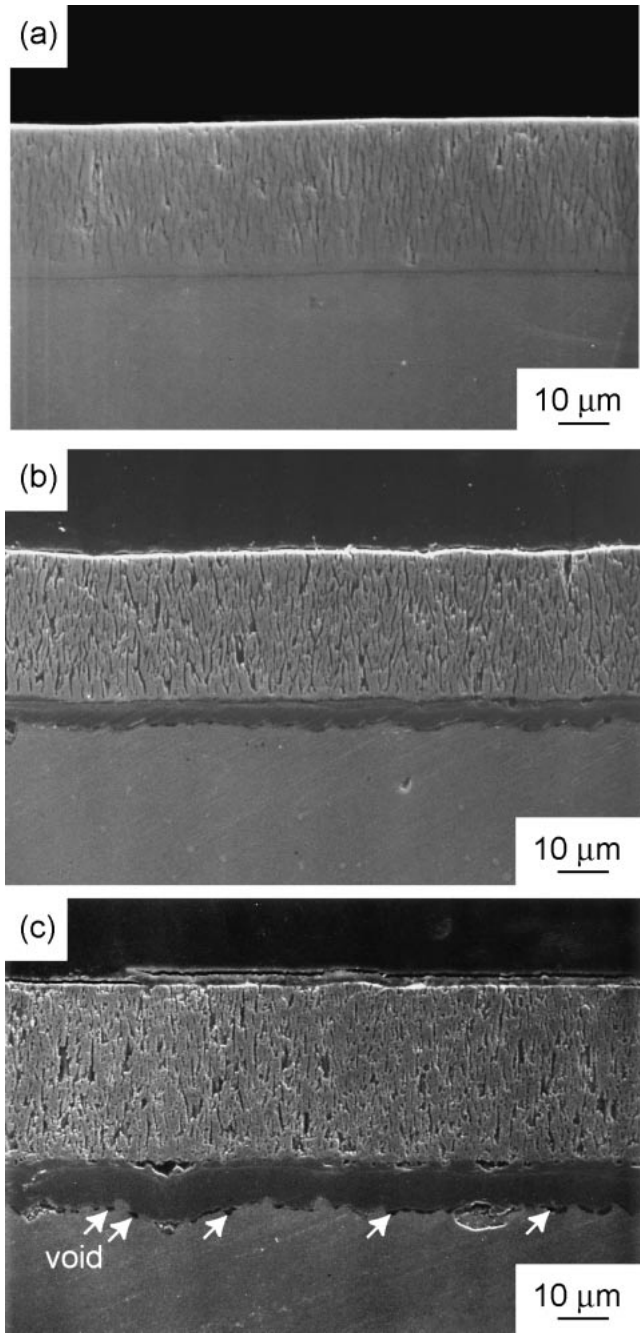

Fig. 8 Cross-sectional views of YSZ coatings on Hastelloy-XR alloys after (a) 20, (b) 500 and (c) 1200 cycles in the 600–1373 K interval in air.

Figure 8 shows cross-sectional views of YSZ coatings containing 4 mol% Y_2O_3 after 20, 500 and 1200 cycles in the 600–1373 K interval. Although the thickness of the TGO layer increased with an increase in the number of thermal cycles, the YSZ coating adhered well to the Hastelloy-XR substrate. The TGO layer consisted of inner Cr_2O_3 and outer $(Ni,Mn,Fe)(Fe,Cr)_2O_4$ spinel layers. This double layer structure was the same as that formed by the oxidation of the Hastelloy-XR alloy.[20)] Many voids were observed at the YSZ/TGO and TGO/Hastelloy-XR interfaces after 1200 cycles (Fig. 8(c)).

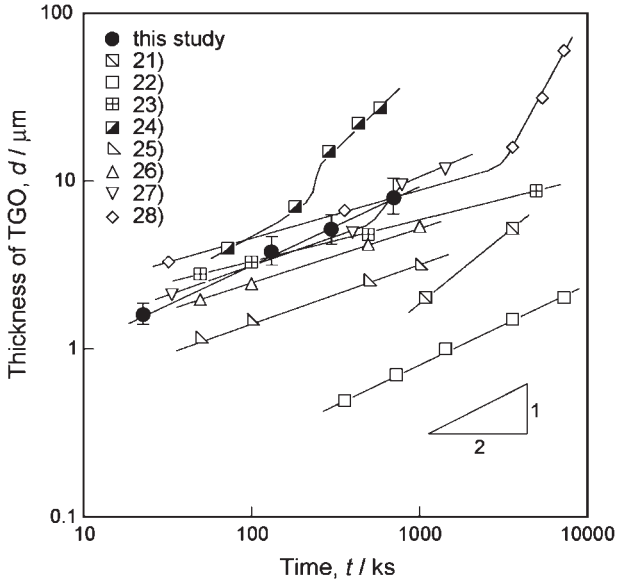

Fig. 9 Relationship between thickness of TGO layer and thermal cycle time for APS, EB-PVD and CVD (this study) YSZ coatings.

The growth of the TGO layer has been widely investigated by using MCrAlY (M: Ni, Co) bond coat layers for EB-PVD and APS YSZ coatings.[21–28] Figure 9 summarizes the relationship between the thickness of the TGO layer and the total net heating time at the maximum temperature of thermal cycle tests in the present study and that in the literatures. The coatings and thermal cycle testing conditions are shown in Table 1. The TGO phase mainly consisted of Cr_2O_3 in the present study because no bond coat layer was applied. However, the TGO phase was Al_2O_3 in EB-PVD and APS YSZ coatings with MCrAlY bond coat layers. The growth rate of Cr_2O_3 in the present TGO layers was almost the same as those of Al_2O_3 in EB-PVD and APS at similar temperature intervals. It is commonly understood that a YSZ coating by APS and EB-PVD may be delaminated after the growth of a TGO layer with a thickness of over 10 μm. However, no delamination was observed in the CVD YSZ coatings in which TGO thickness was around 10 μm.

Figures 10(a) and (b) show the surface and cross-sectional views of partially delaminated CVD YSZ coatings containing 0.5 mol% Y_2O_3 after 1200 cycles in the 600–1373 K interval. Figures 10(a) and (b) indicate that the YSZ coating was

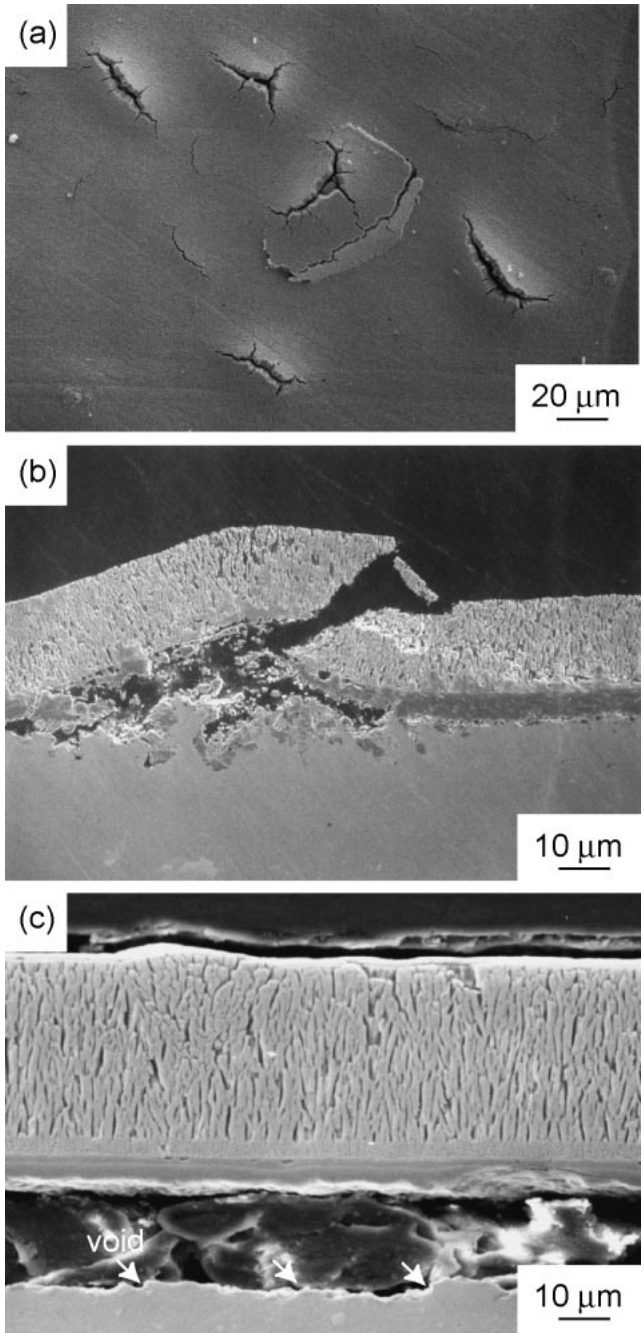

Fig. 10 Surface and cross-sectional views of partially and wholly delaminated YSZ coatings after 1200 cycles in the 600–1373 K interval.

Table 1 Preparation and thermal cycle testing conditions as reported in the literature.

Preparation Method	Substrate	Temperature (K)	Holding-cooling time (ks)	Reference
MO-CVD	Hastelloy-XR	1373	0.6–0.6	This study
EB-PVD	NiCoCrAlYRe/PWA1483	1223	Static	21)
EB-PVD	NiCoCrAlY/IN738	1323	7.2–0.9	22)
EB-PVD	NiCoCrAlY/Rene142	1373	3–0.6	23)
EB-PVD	PtAl/ReneN5	1450	2.7–0.6	24)
PS	NiCoCrAlY/Ni superalloy	1223	Static	25)
PS	NiCoCrAlY/IN738	1323	Static	26)
PS	NiCoCrAlY/CMSX-4	1394	3–0.6	27)
PS	NiCoCrAlY/Haynes230	1323	360–6.9	28)

partially cracked after the thermal cycles. The cracks might be caused by bending stress accompanying with the blistering due to localized interfacial oxidation. The fracture of the YSZ coating at an angle of about 45° suggests that shearing compressive stress may be associated with cracking during the cooling process. Therefore, the YSZ coating failure might be caused by the combination of bending stress and shearing compressive stress. Figure 10(c) shows a cross-sectional view of a wholly delaminated YSZ coating containing 9.5 mol% Y_2O_3 after 1200 cycles in the 600–1373 K interval. A thin Hastelloy-XR layer lay under the TGO layer, and many voids were observed at the cracked Hastelloy-XR surface. It is known that the oxidation of Hastelloy-XR alloy proceeds by the outward diffusion of Cr ions, leaving voids (Kirkendall voids) inside this alloy.[20] The trace of voids can be observed as indicated by arrows in Fig. 10(c). The voids would lower the adherence between the TGO layer and Hastelloy-XR, and easily result in delamination by compressive stress. It has also been reported that the voids formed at the interface between a MCrAlY bond coat and the TGO layer could cause delamination in APS (or EB-PVD) YSZ coatings.[29,30]

4. Conclusions

The effect of Y_2O_3 content on thermal cycle resistance of YSZ coatings prepared by MO-CVD was investigated. The YSZ coatings containing 4 mol% Y_2O_3 showed no delamination after 1200 cycles in the 600–1373 K interval. The structure of the YSZ coating containing 4 mol% Y_2O_3 was tetragonal in a single phase, and no phase transformation was identified after the thermal cycle tests. The TGO layers consisting of inner Cr_2O_3 and outer $(Ni,Mn,Fe)(Fe,Cr)_2O_4$ spinel increased with increasing thermal cycle time, and the YSZ coatings were still adhered to the alloy after the growth of a TGO layer with a thickness of around 10 μm. The delamination of YSZ coatings occurred at the Hastelloy-XR alloy side near the interface between the alloy and the TGO layer. Many Kirkendall voids were observed at the delaminated surface.

Acknowledgement

This work was performed as a part of the Nanostructure Coating Project carried out by the New Energy and Industrial Technology Development Organization (NEDO), Japan.

REFERENCES

1) W. Beele, G. Marijnissen and A. van Lieshout: Surf. Coat. Technol. **120–121** (1999) 61–67.
2) A. G. Evans, D. R. Mumm, J. W. Hutchinson, G. H. Meier and F. S. Pettit: Prog. Mater. Sci. **46** (2001) 505–553.
3) J. Thornton: Mater. Forum **22** (1998) 159–181.
4) U. Schulz and M. Schmücker: Mater. Sci. Eng. A **276** (2000) 1–8.
5) C. Leyens, U. Schulz, B. A. Pint and I. G. Wright: Surf. Coat. Technol. **120–121** (1999) 68–76.
6) S. P. Krumdieck, O. Sbaizero, A. Bullert and R. Raj: Surf. Coat. Technol. **167** (2003) 226–233.
7) M. Krellmann, D. Selbmann, U. Schmatz and F. Weiss: J. Alloy. Compd. **251** (1997) 307–309.
8) H. Yamane and T. Hirai: J. Mater. Sci. Lett. **6** (1987) 1229–1230.
9) E. Sipp, F. Langlais and R. Naslain: J. Alloy. Compd. **186** (1992) 65–76.
10) Y. Akiyama, T. Sato and N. Imaishi: J. Crys. Growth **147** (1995) 130–146.
11) M. Pulver, W. Nemetz and G. Wahl: Surf. Coat. Technol. **125** (2000) 400–406.
12) G. Wahl, W. Nemetz, M. Giannozzi, S. Rushworth, D. Baxter, N. Archer, F. Cernuschi and N. Boyle: Trans. ASME **123** (2001) 520–524.
13) R. Tu, T. Kimura and T. Goto: Mater. Trans. **43** (2002) 2354–2356.
14) R. Tu, T. Kimura and T. Goto: Surf. Coat. Technol. **187** (2004) 238–244.
15) T. K. Gupta, F. F. Lange and J. H. Bechtold: J. Mater. Sci. **13** (1978) 1464–1470.
16) R. C. Garvie: J. Phys. Chem. **69** (1965) 1238–1243.
17) H. G. Scott: J. Mater. Sci. **10** (1975) 1527–1535.
18) E. H. Kisi and C. J. Howard: Key Eng. Mater. **153–154** (1998) 1–36.
19) A. H. Heuer, R. Chaim and V. Lanteri: *Advances in Ceramics: Science and Technology of Zirconia III*, Vol. 24, A. S. Somiya *et al.*, eds., (American Ceramics Society, Cleveland, Ohio, 1988, pp. 3–20.
20) R. Tu and T. Goto: J. Mater. Sci. Technol. **19** (2003) 19–22.
21) N. Czech, H. Fietzek, M. Juez-Lorenzo and V. Kolarik: Surf. Coat. Technol. **113** (1999) 157–164.
22) D. Strauss, G. Muller, G. Schumacher, V. Engelko, W. Stamm, D. Clemens and W. J. Quaddakers: Surf. Coat. Technol. **135** (2001) 196–201.
23) U. Schulz, M. Menzebach, C. Leyens and Y. Yang: Surf. Coat. Technol. **146–147** (2001) 117–123.
24) S. Q. Nusier, G. M. Newaz and Z. A. Chaudhury: Int. J. Solids Struct. **37** (2000) 2495–2506.
25) E. P. Busso, J. Lin, S. Sakurai and M. Nakayama: Acta Mater. **49** (2001) 1515–1528.
26) S. Widjaja, A. M. Limarga and T. H. Yip: Mater. Lett. **57** (2002) 628–634.
27) K. W. Schlichting, N. P. Padture, E. H. Jordan and M. Gell: Mater. Sci. Eng. A **342** (2003) 120–130.
28) M. S. Ali, S. Song and P. Xiao: J. Eur. Cera. Soc. **22** (2002) 101–107.
29) Y. H. Sohn, J. H. Kim, E. Jordan and M. Gell: Surf. Coat. Technol. **146–147** (2001) 70–78.
30) B. A. Pint: Oxid. Met. **48** (1997) 303–328.